Charge Transfer Kinetics in Thin-Film Voltammetry. Theoretical Study under Conditions of Square-Wave Voltammetry

ARTICLE *in* THE JOURNAL OF PHYSICAL CHEMISTRY B · JUNE 2004

Impact Factor: 3.3 · DOI: 10.1021/jp0487152

1 AUTHOR:

Valentin Mirceski
Ss. Cyril and Methodius University

102 PUBLICATIONS **1,600** CITATIONS

SEE PROFILE

Charge Transfer Kinetics in Thin-Film Voltammetry. Theoretical Study under Conditions of Square-Wave Voltammetry

Valentin Mirčeski[†]

Institute of Chemistry, Faculty of Natural Sciences and Mathematics, "Sts. Cyril and Methodius" University, P.O. Box 162, 1000 Skopje, Republic of Macedonia

Received: March 23, 2004; In Final Form: April 27, 2004

An electrode reaction controlled by charge transfer kinetics and occurring in a finite diffusion space is theoretically studied under conditions of square-wave voltammetry (SWV). A simple numerical solution is derived based on the modified step-function method (Mirčeski, V. *J. Electroanal. Chem.* **2003**, *545*, 29). The SW voltammetric response is mainly controlled by the thickness parameter $\Lambda = L\sqrt{(f/D)}$, the redox kinetic parameter $K = k_s/\sqrt{Df}$, and the electron transfer coefficient α, where L is the thickness of the film, k_s is the heterogeneous standard redox rate constant, f is the frequency of the potential modulation, and D is the diffusion coefficient of the electroactive species. The mass transport regime is predominantly determined by the thickness parameter. The typical interval for finite diffusion is $\log(\Lambda) \leq 0.3$. The main properties of the electrode reaction occurring in a finite diffusion space are the quasireversible maximum and the splitting of the net SW peak. The quasireversible maximum is manifested as a parabola-like dependence of the dimensionless net peak current on the redox kinetic parameter. The maximum of this dependence, which is positioned within the quasireversible region, is selectively sensitive to the standard redox rate constant, for a given thickness of the film. For a large amplitude of the potential modulation, the net SW response splits into two peaks that are positioned symmetrically around the formal potential of the redox system. The splitting is attributed to the fast electrode reactions. The separation between the split peaks is sensitive to both the SW amplitude and the redox kinetic parameter, whereas the relative heights of the split peaks are solely determined by the electron transfer coefficient. Both properties, the quasireversible maximum and the splitting of the net SW peak, can be exploited for complete kinetic characterization of the system and accurate determination of the formal potential of the quasireversible electrode reaction by a fast and simple experimental procedure.

1. Introduction

The application of thin-film voltammetry for studying charge transfer reactions of biological significance has increased rapidly in the past decade.[1−33] The redox properties of biological macromolecules such as enzymes and proteins are almost inaccessible when these molecules are dissolved in the electrolyte solution. Thus, formation of a protein thin film on a solid electrode surface is necessary to promote the electron transfer between the electrode and the electroactive protein.[1−4] In most of the cases the biological macromolecules undergo a slow interfacial electron transfer, the kinetics of which can be partly enhanced by modifying the electrode surface with a polymer film, various surfactants, or lipid-like molecules, mediating the interfacial electron transfer to or from the target molecules.[4−14] Even in such cases, the overall electrode reaction undergoes a quasireversible surface electrode process or a process occurring in a restricted diffusion space. Furthermore, the knowledge of the redox kinetics of processes occurring in a finite diffusion space is of crucial importance for several other areas in which polymer-modified electrodes are applied, such as light emitting diodes, biofuel cells, superior metal-cantered catalysis, and electron organic synthesis.[15−20]

Thin-film voltammetry has been recently proposed as an effective and simple method for studying charge transfer across the liquid interface with the use of the conventional three-electrode voltammetric cell.[21−33] Anson et al.[21−26] used a solid graphite electrode the surface of which was completely covered with a thin film of a water-immiscible organic liquid containing an electroactive probe. This method possesses a number of advantages, and it is particularly useful for studying electron transfer across the liquid interface with a simple experimental arrangement.[23] Later, Scholz et al. developed three-phase electrodes as a powerful tool for measuring the Gibbs energy of ion transfer across the liquid interface.[27−33] The three-phase electrodes enabled the study of ion transfer reactions of miscellaneous inorganic ions and a series of biologically important organic ions that have been inaccessible so far by the conventional four-electrode voltammetric arrangement. In a recent study,[34] it has been demonstrated that the voltammetric properties of three-phase electrodes can also be explained on the basis of thin-film voltammetry.

Besides cyclic voltammetry,[35−37] square-wave voltammetry (SWV) is the second powerful voltammetric tool for studying both the mechanism and kinetics of electrode reactions in a thin film.[38,39] Because it is one of the most advanced voltammetric techniques,[39] the usefulness of SWV for studying the electrode reactions occurring in restricted diffusion conditions has been proven in particular with three-phase electrodes.[27−34] Nevertheless, to the best of our knowledge, the effect of charge transfer kinetics in thin-film square-wave voltammetry has not been studied so far. With this motivation, a detailed theoretical study of the quasireversible electrode reaction occurring in limiting diffusion space is presented under conditions of SWV. Special

[†] E-mail: valentin@iunona.pmf.ukim.edu.mk. Phone: ++ 389 70 83 64 63. Fax: ++ 389 2 3226 865.

10.1021/jp0487152 CCC: $27.50
Published on Web 06/11/2004

TABLE 1: List of Symbols and Abbreviations

symbol	meanings of the symbols and abbreviations	units
α	cathodic electron transfer coefficient	1
c_{Ox}	concentration of the oxidized form	mol cm^{-3}
c_{Red}	concentration of the reduced form	mol cm^{-3}
c^*_{Ox}	initial concentration of the oxidized form in the film	mol cm^{-3}
D	diffusion coefficient	cm^2 s^{-1}
d	main time increment	s
d'	subtime increment	s
dE	scan increment	mV
$E^0_{Ox/Red}$	standard redox potential	V
f	square-wave frequency	s^{-1}
f_{max}	frequency associated with the position of the quasireversible maximum	s^{-1}
F	Faraday constant	C/mol
φ	dimensionless potential	1
I	current	A
ΔI_p	net peak current	A
K	dimensionless kinetic parameter	1
k_s	heterogeneous standard redox rate constant	cm s^{-1}
L	thickness of the film	cm
Λ	dimensionless thickness parameter	1
R	gas constant	J mol^{-1} K^{-1}
S	electrode surface area	cm^2
t	time	s
T	thermodynamic temperature	K
x	distance	cm
Ψ	dimensionless current	1
$\Delta\Psi_p$	dimensionless net peak current	1

attention is paid to the properties of the SW voltammetric response that can serve for a simple assessment of the redox kinetics of the electrode reaction.

2. Mathematical Model

The quasireversible reaction of two chemically stable species, occurring in a thin film with a thickness L, is investigated:

$$\mathrm{Ox} + n\mathrm{e}^- \rightleftarrows \mathrm{Red} \qquad \text{(I)}$$

For simplicity, the charge of the species is omitted and the diffusion coefficients of both Ox and Red are assumed to be equal. The following model represents mathematically the electrode reaction:

$$\frac{\partial c_{Ox}}{\partial t} = D\frac{\partial^2 c_{Ox}}{\partial x^2} \qquad (1)$$

$$\frac{\partial c_{Red}}{\partial t} = D\frac{\partial^2 c_{Red}}{\partial x^2} \qquad (2)$$

$$t = 0,\ 0 \le x \le L: \quad c_{Ox} = c^*_{Ox},\ c_{Red} = 0 \qquad (3)$$

$$t > 0,\ x = 0: \quad \left(\frac{\partial c_{Ox}}{\partial x}\right) = -\left(\frac{\partial c_{Red}}{\partial x}\right) = \frac{I}{nFDS} \qquad (4)$$

$$t > 0,\ x = L: \quad D\left(\frac{\partial c_{Red}}{\partial x}\right) = -D\left(\frac{\partial c_{Ox}}{\partial x}\right) = 0 \qquad (5)$$

$$\frac{I}{nFS} = k_s \exp(-\alpha\varphi)[(c_{Ox})_{x=0} - \exp(\varphi)(c_{Red})_{x=0}] \qquad (6)$$

$$\varphi = \frac{nF}{RT}(E - E^0_{Ox/Red}) \qquad (7)$$

Here, k_s is the standard heterogeneous redox rate constant in units of cm s^{-1} and α is the cathodic electron transfer coefficient. For the meaning of all other symbols and abbreviations see Table 1. The differential equations 1 and 2 have been solved with the aid of Laplace transforms. The numerical solution has been derived by the recently introduced modified step-function method as described in ref 40. The solution is represented by the following recursive formula:

$$\Psi_m = \frac{K\exp(-\alpha\varphi_m)\left[1 + \dfrac{(1+\exp(\varphi_m))}{50p\sqrt{f}}\displaystyle\sum_{j=1}^{m-1}\Psi_j S_{m-j+1}\right]}{1 - K\exp(-\alpha\varphi_m)(1+\exp(\varphi_m))\dfrac{S_1}{50p\sqrt{f}}} \qquad (8)$$

Here the dimensionless current is defined as $\Psi = I/(nFSc^*_{Ox}\sqrt{Df})$ and K is the dimensionless redox kinetic parameter defined as $K = (k_s/\sqrt{(Df)})$. For the derivation of eq 8 both variables, the current I and time t, were discretized. To each time $t = md$, where d is a time increment and m is the serial number, a certain current I_m was ascribed. The serial number m ranges from 1 to N, where N is the maximal number of time increments fulfilling the conditions $t_{tot} = Nd$ and t_{tot} is the total time of the voltammetric experiment. The main time increment was defined as $d = 1/(50f)$, where f is the frequency of the potential modulation. This means that each pulse of the potential modulation was divided into 25 time increments. The integration factor is $S_m = \sum_{i=p(m-1)}^{pm}\Phi_i$. The discrete values of the function Φ_i are calculated according to the following recursive formula:

$$\Phi_i = \frac{\dfrac{1}{\sqrt{\pi i d'}} + \dfrac{\exp\left(\dfrac{-a^2}{4id'}\right)}{\sqrt{\pi i d'}} - \displaystyle\sum_{j=1}^{i-1}\Phi_i M_{i-j+1}}{M_1 - 1} \qquad (9)$$

where $M_i = erfc(a/(2\sqrt{(i+1)d'})) - erfc(a/(2\sqrt{(id')}))$, and $a = 2(L/\sqrt{D})$. For the derivation of formula 9, each main time increment was divided into p subtime intervals. The subtime increment was defined as $d' = (d/p)$. In this work the number of subintervals is set to $p = 5$. Thus the serial number i ranges from 1 to Np.

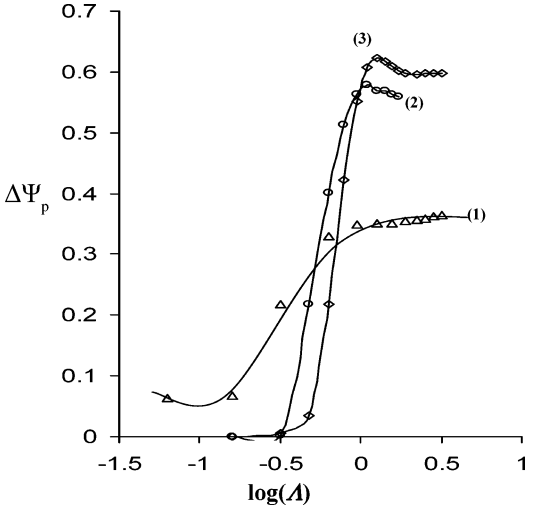

Figure 1. Dependence of the dimensionless net SW peak currents on the logarithm of the thickness parameter Λ for different redox kinetic parameters. The redox kinetic parameter was $\log(K) = -0.6$ (1), 0 (2), and 0.6 (3). The other conditions of the simulations were amplitude $nE_{sw} = 50$ mV, scan increment $dE = 10$ mV, and electron transfer coefficient $\alpha = 0.5$.

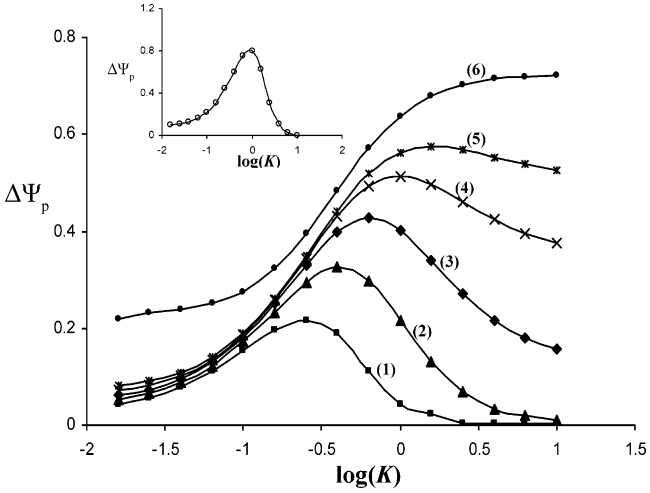

Figure 2. Dependence of the dimensionless net SW peak currents on the logarithm of the redox kinetic parameter K for different thicknesses of the thin film. The thickness parameter was $\log(\Lambda) = -0.50$ (1), -0.33 (2), -0.20 (3), -0.10 (4), and -0.02 (5). Curve 6 corresponds to the quasireversible electrode reaction under semi-infinite diffusion conditions.[39] The inset shows the corresponding dependence in the case of a diffusionless surface electrode reaction. The other conditions of the simulations were amplitude $nE_{sw} = 50$ mV, scan increment $dE = 10$ mV, and electron transfer coefficient $\alpha = 0.5$.

It is worth emphasizing that the final numerical solution of the complex mathematical problem defined by eqs 1−7 is represented by two simple recursive formulas (eqs 8 and 9) demonstrating the advantages of the modified step-function method.[40]

3. Results and Discussion

3.1. The Influence of the Thickness of the Film on the Mass Transport Regime. The influence of the charge transfer kinetics and the diffusion mass transport in thin-film voltammetry is controlled by two crucial dimensionless parameters: the redox kinetic parameter $K = (k_s/\sqrt{(Df)})$ and the thickness parameter $\Lambda = L\sqrt{(f/D)}$, respectively. As indicated by the redox kinetic parameter, the overall effect of the charge transfer kinetics depends on the rate of the electron exchange, the diffusion mass transport, and the time-window of the voltammetric experiment. The dimensionless thickness parameter unifies the actual thickness of the thin layer L with the diffusion coefficient and the time-window of the voltammetric experiment, determining predominantly the mass transport regime within the thin film. Depending on Λ, the electrode reaction can appear as a surface process,[39,41,42] an electrode reaction controlled by restricted diffusion, or a simple electrode reaction occurring under semi-infinite diffusion conditions.[39] The effect of the thickness parameter on the dimensionless net SW peak current is presented in Figure 1. The relationship between the peak current $\Delta\Psi_p$ and the thickness parameter Λ is sigmoidal for any kinetics of the electrode reaction. The ascending part of the sigmoidal curve corresponds to an electrode reaction occurring under restricted diffusion conditions. The lower plateau of the curve is typical for diffusionless conditions, i.e., the thickness of the film is smaller than the thickness of the diffusion layer developed during the voltammetric experiment causing a full exhaustion of the electroactive material in the thin film. Under such conditions, the voltammetric behavior of the system is equivalent to the surface electrode reaction. On the other hand, the upper plateau of the curves in Figure 1 refers to an electrode reaction controlled by a semi-infinite diffusion mass transport regime.

The wideness of the restricted diffusion region depends partly on the redox kinetic parameter. Increasing the rate of the electron exchange extends slightly the interval of Λ values under which the limiting diffusion occurs as a consequence of the increasing thickness of the diffusion layer. For instance, for $\log(K) = -0.6$ the restricted diffusion is associated with the interval $\log(\Lambda) \leq 0.2$ (see curve 1 in Figure 1), whereas for $\log(K) = 0.6$ the corresponding interval is $\log(\Lambda) \leq 0.4$ (see curve 3 in Figure 1).

It is important to note that studying a single experimental system, characterized with constant values of L and D, the regime of mass transport can be varied by the frequency of the potential modulation. For instance, for a thin layer of 5 μm and diffusivity of $D = 1 \times 10^{-5}$ cm^2 s^{-1}, the variation of the SW frequency from 1 to 1000 s^{-1} results in the variation of Λ within the interval $-0.8 \leq \log(\Lambda) \leq 0.7$. This means that the system can be easily transposed from the conditions of surface-like behavior up to conditions typical for semi-infinite diffusion.

3.2. Quasireversible Maximum in Thin-Film Voltammetry. Figure 2 depicts the dependence of the dimensionless peak current on the logarithm of the redox kinetic parameter. Interestingly, within the quasireversible region, the dimensionless peak current depends nonlinearly on the redox kinetic parameter forming a well-developed maximum. As the electrode reaction approaches the conditions of semi-infinite diffusion, the parabola-like dependence is lost transforming into a sigmoidal curve (see curves 5 and 6 in Figure 2). The parabola-like dependence accompanies the electrode reaction occurring in restricted diffusion space (see curves 1−4 in Figure 2) as well as a diffusionless surface electrode reaction[42] (see the inset of Figure 2). Obviously, this effect is a consequence of a combined simultaneous influence of the redox kinetic parameter K and thickness parameter Λ. In other words, the effect is a consequence of the slow electron transfer of an electrode reaction occurring in restricted diffusion space.

The parabola-like dependence of the net SW peak current on the redox kinetic parameter could be called the "quasireversible maximum" by analogy with the well-known property of the wide class of adsorption-coupled electrode reactions.[39,42−49] The importance of the quasireversible maximum stems from the fact that it can be exploited for estimation of the charge

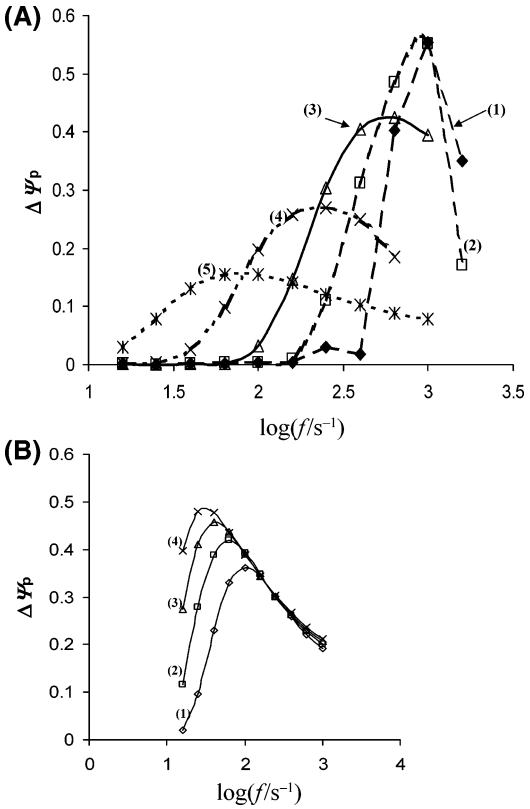

Figure 3. Quasireversible maxima calculated by altering the frequency of the potential modulation for different standard redox rate constants (A) and different thicknesses of the film (B). The conditions corresponding to A were heterogeneous standard rate constant $\log(k_s/\mathrm{cm\ s^{-1}}) = -1.5$ (1), -2 (2), -2.5 (3), -3 (4), and -3.5 (5). The thickness of the film was 1 μm. The conditions corresponding to B were the thickness of the film $L/\mu\mathrm{m} = 2$ (1), 3 (2), 4 (3), and 5 (4). The heterogeneous standard rate constant was $\log(k_s/\mathrm{cm\ s^{-1}}) = -3$. The other conditions of the simulations for both A and B were electron transfer coefficient $\alpha = 0.5$, amplitude $nE_{sw} = 50$ mV, scan increment $dE = 10$ mV, and diffusion coefficient $D = 1 \times 10^{-5}$ cm^2 s^{-1}.

transfer kinetics by a fast and simple experimental procedure.[43,44,48,49] The first experimental indication for the presence of the quasireversible maximum in the case of thin-film voltammetry was observed in the recent experiments with azobenzene at the three-phase electrodes.[34]

The quasireversible maximum is a consequence of the specific chronoamperometric properties of the electrode reaction occurring in restricted diffusion space and the current sampling procedure used in SWV.[39] For a quasireversible electrode reaction, when the rate of the electron exchange is synchronized with the duration of the single potential pulse of the SW potential modulation (frequency of the potential modulation), the highest current is measured at the end of the pulse. For a reversible electrode reaction a large current is produced at the beginning of the SW pulse. Nevertheless, the current steeply decreases in the course of the potential pulse due to the exhaustion of the thin film with the electroactive material and a rapid restoration of the redox equilibrium at the electrode surface. Consequently, at the end of the SW pulse a minute current remains to be measured. For these reasons, the net SW peak current of a reversible electrode reaction is significantly lower than that of a quasireversible reaction.

Both the quasireversible region of the electrode reaction and the position of the quasireversible maximum depend on the thickness of the film. As the thickness of the film increases, the quasireversible maximum is shifted toward faster electrode reactions (compare curves 1−4 in Figure 2). By analogy with the surface electrode reactions,[42] the position of the quasireversible maximum can be attributed with a certain critical value of the redox kinetic parameter K_{max}. Thus, the critical value of the redox kinetic parameter is a function of the film thickness. For SW amplitude $nE_{sw} = 50$ mV, and scan increment of $dE = 5$ mV, the following relationship was found: $\log(K_{max}) = 1.2649\Lambda - 1$ with a linear regression coefficient $R = 1$. In addition, the critical parameter K_{max} is also a function of the amplitude of the potential modulation. The increase of the amplitude causes the shift of the quasireversible maximum toward lower K_{max} values. The corresponding dependence is associated with the following equation: $\log(K_{max}) = -0.007(nE_{sw}/\mathrm{mV}) + 0.16$ ($R = 0.971$), which holds for $\log(\Lambda) = -0.2$ and $dE = 10$ mV. Interestingly, in contrast to the surface electrode reaction,[42] the critical redox kinetic parameter does not depend on the electron transfer coefficient.

TABLE 2: Linear Regression Functions Representing the Dependence of the Standard Heterogeneous Standard Redox Rate Constant on the Critical Frequency for Different Thicknesses of the Film[a]

L/μm	linear equation	R
1	$\log(k_s/\mathrm{cm\ s^{-1}}) = 0.0015(f_{max}/\mathrm{s^{-1}}) - 3.4971$	0.99
2	$\log(k_s/\mathrm{cm\ s^{-1}}) = 0.0039(f_{max}/\mathrm{s^{-1}}) - 2.502$	0.98
3	$\log(k_s/\mathrm{cm\ s^{-1}}) = 0.0098(f_{max}/\mathrm{s^{-1}}) - 2.6656$	0.99
4	$\log(k_s/\mathrm{cm\ s^{-1}}) = 0.0119(f_{max}/\mathrm{s^{-1}}) - 2.4777$	0.99
5	$\log(k_s/\mathrm{cm\ s^{-1}}) = 0.0286(f_{max}/\mathrm{s^{-1}}) - 2.8276$	0.99
6	$\log(k_s/\mathrm{cm\ s^{-1}}) = 0.0621(f_{max}/\mathrm{s^{-1}}) - 3.4908$	0.99
7	$\log(k_s/\mathrm{cm\ s^{-1}}) = 0.0441(f_{max}/\mathrm{s^{-1}}) - 2.8904$	0.99
8	$\log(k_s/\mathrm{cm\ s^{-1}}) = 0.0789(f_{max}/\mathrm{s^{-1}}) - 3.2087$	0.99

[a] The conditions of the simulations were amplitude $nE_{sw} = 50$ mV, scan increment $dE = 10$ mV, electron transfer coefficient $\alpha = 0.5$, and diffusion coefficient 1×10^{-5} cm^2 s^{-1}.

The theoretical analysis presented in Figure 2 corresponds to a comparison of a series of electrode reactions characterized with different redox kinetics occurring in films of equal thickness. Among them, there is a single electrode reaction exhibiting the highest net SW response, which represents the physical meaning of the quasireversible maximum. Such an electrode reaction is characterized with a standard redox rate constant and the diffusion coefficient fulfilling the condition $(k_s/\sqrt{(Df)}) = K_{max}$. Nevertheless, in experimental reality, instead of comparing different reactions, one is interested much more in inspecting a single electrode reaction. In this case, the redox kinetic parameter K can be varied by adjusting the signal frequency only, since both the standard redox rate constant k_s and diffusion coefficient D are typical constants for a particular electrode reaction. However, the variation of the SW frequency affects simultaneously both the redox kinetic parameter $K = (k_s/\sqrt{(Df)})$ and the thickness parameter $\Lambda = L\sqrt{(f/D)}$. Thus, the effect of the frequency is expected to be much more complicated than the previous sole dependencies on K and Λ.

Figure 3 depicts the dependence of the dimensionless net SW peak current on the logarithm of the signal frequency for different redox rate constants (Figure 3A) and different thicknesses of the film (Figure 3B). These analyses clearly confirmed that the quasireversible maximum could be constructed by varying the SW frequency, and its position is sensitive to the redox kinetics of the electrode reaction (see Figure 3A). When the logarithm of the standard rate constant was plotted versus the critical frequency f_{max}, i.e., the frequency at which the quasireversible maximum is reached, a linear relation was found. The slope and the intercept of the line depend slightly on the particular thickness of the film, as implied by the analysis in Figure 3B. Table 2 lists the linear functions representing the relationship $\log(k_s)$ versus f_{max} for a series of film thickness.

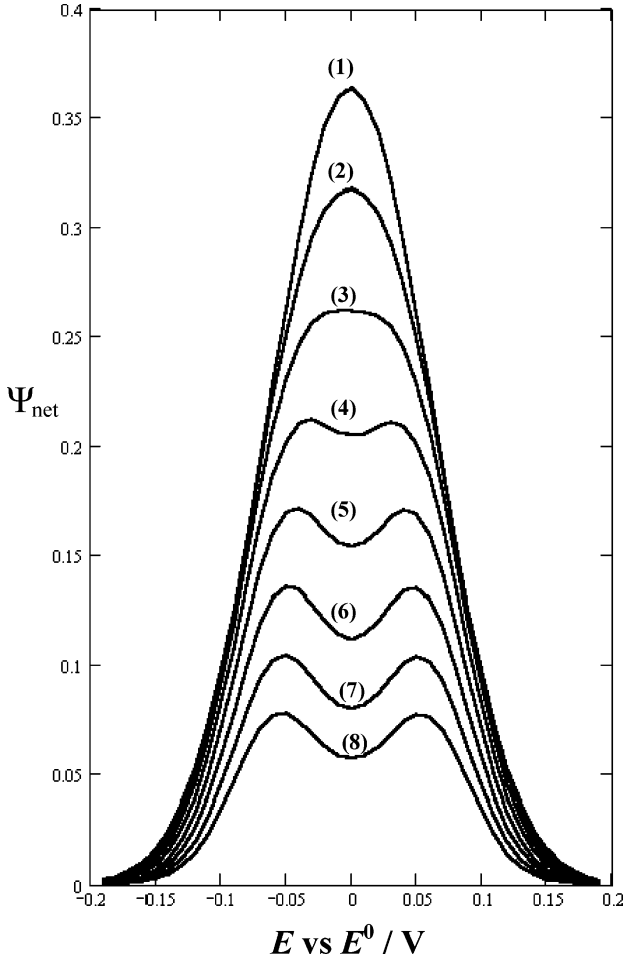

Figure 4. Splitting of the net SW response under influence of the redox kinetic parameter. The redox kinetic parameter was $\log(K) = -0.4$ (1), -0.3 (2), -0.2 (3), -0.1 (4), 0 (5), 0.1 (6), 0.2 (7), and 0.3 (8). The other conditions of the simulations were thickness parameter $\log(\Lambda) = -0.32$, electron transfer coefficient $\alpha = 0.5$, amplitude $nE_{sw} = 80$ mV, and scan increment $dE = 10$ mV.

In real experiments one analyses the real net SW peak current ΔI_p as a function of the frequency. The ratio of the real peak current and the square root of the corresponding frequency ($\Delta I_p/\sqrt{f}$) corresponds to the dimensionless peak current $\Delta\Psi_p$ ($\Delta\Psi_p = \Delta I_p/(nFSc^*_{Ox}\sqrt{(Df)})$). Thus, plotting the ratio $\Delta I_p/\sqrt{f}$ versus $\log(f)$ one obtains an analogous dependence as those presented in Figure 3. The critical frequency f_{max} associated with the position of the experimentally measured quasireversible maximum reveals the standard redox rate constant with the aid of the equations given in Table 2. Note that Table 2 gives only a few examples covering a narrow interval of possible experimental conditions. For specific set of experimental conditions, one can easily construct an appropriate calibration line by calculating the theoretical response with the aid of recursive formulas 8 and 9.

The important advantage of the quasireversible maximum is that for a given film thickness it is almost exclusively sensitive to the standard redox rate constant. One does not require knowledge of the electron transfer coefficient to estimate the kinetics of the electron transfer, which is the case in other voltammetric methods. The drawback of this method follows from the fact that it is related with thin films only. For films thicker that 10 μm, one can easily transpose the electrode reaction into semi-infinite diffusion conditions by increasing the frequency, causing vanishing of the quasireversible maximum. For instance, for $L = 10$ μm and $D = 1 \times 10^{-5}$ cm^2 s^{-1}, one is limited to varying the frequency over the interval $f \leq 20$ s^{-1}, which could be insufficient for redox kinetic measurements.

3.3. Splitting of the Net SW Peak. Apart from the quasireversible maximum, the second remarkable property of the thin-film SW voltammetric response is the splitting of the net SW peak under a large amplitude of the potential modulation. Similar to the surface electrode reactions,[41] the splitting of the net SW response is associated with the fast electrode reaction, characterized with the large redox kinetic parameter. Figure 4 depicts the influence of the redox kinetic parameter on the shape of the net SW responses of an electrode reaction occurring in a film with thickness $\log(\Lambda) = -0.32$. As the apparent reversibility of the reaction increases the single net SW peak commences splitting. Once split, the potential separation between the split peaks increases in proportion to the redox kinetic parameter. Figure 5 illustrates the origin of the splitting

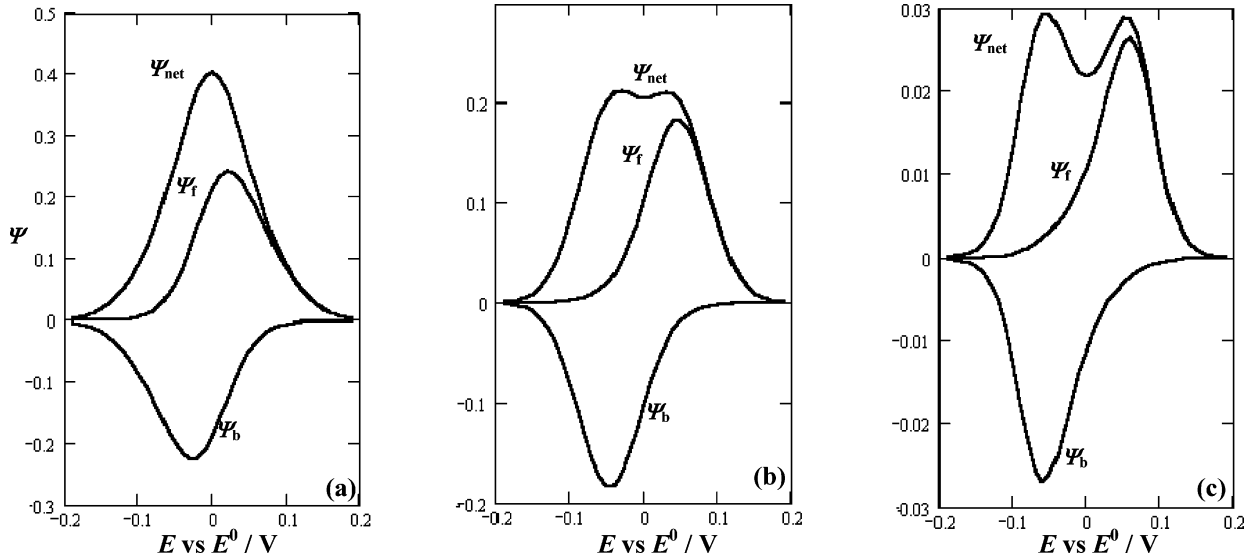

Figure 5. The effect of the redox kinetic parameter to all components of the SW voltammetric response of an electrode reaction occurring in a film with thickness parameter $\log(\Lambda) = -0.324$. The redox kinetic parameter was $\log(K) = -0.6$ (a), -0.1 (b), and 0.6 (c). The other conditions of the simulations were amplitude $nE_{sw} = 80$ mV, scan increment $dE = 10$ mV, and electron transfer coefficient $\alpha = 0.5$. The subscripts net, f, and b, correspond to the net, forward, and backward components of the SW response, respectively.

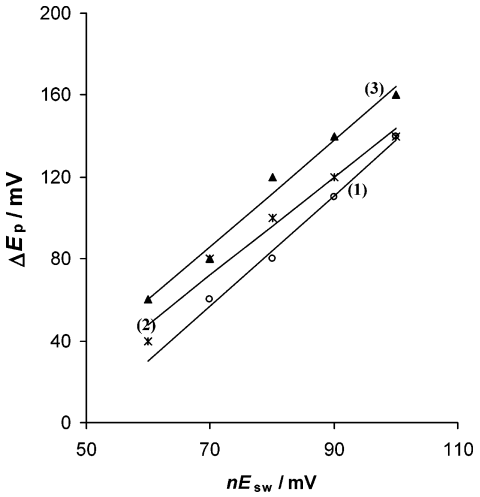

Figure 6. Dependence of the potential separation between the split SW peaks on the amplitude for different redox kinetic parameters. The redox kinetic parameter was $\log(K) = 0$ (1), 0.2 (2), and 0.4 (3). The other conditions of the simulations were thickness parameter $\log(\Lambda) = -0.324$, electron transfer coefficient $\alpha = 0.5$, and scan increment $dE = 10$ mV.

TABLE 3: Intervals of the Redox Kinetic Parameter Values under Which the Splitting of the Response Exists, for Different Thicknesses of the Thin Film[a]

$nE_{sw} = 80$ mV	
$\log(\Lambda)$	$\log(K)$
−0.597	> −0.5
−0.547	> −0.5
−0.500	> −0.4
−0.801	> −0.2
−0.324	> −0.1
−0.199	> 0.2
−0.102	no splitting

[a] The conditions of the simulations were scan increment $dE = 10$ mV and electron transfer coefficient $\alpha = 0.5$.

of the net SW peak. As the reversibility of the electrode reaction increases the separation of the forward and backward components of the SW response enhances causing splitting of the net SW peak. Note that the split SW peaks are symmetrically positioned around the formal potential of the redox system, hence permitting accurate determination of its value. Furthermore, the forward (cathodic) component of the response is positioned at more positive potential in respect to the formal potential of the system. The opposite is valid for the backward (oxidation) component. Such inverse position of both SW components is opposite to the response of an electrode reaction under semi-infinite diffusion,[39] which can serve as a simple criterion for qualitative recognition of the thin-film electrode reaction.

Besides the redox kinetic parameter, the splitting is affected by the thickness of the film. For a particular amplitude, the splitting appears for a critical set of the redox kinetic and thickness parameter values. Table 3 lists the intervals of the redox kinetic parameter values, under which the splitting appears, for different thicknesses of the thin film. Obviously, the splitting is typical for thin films, and the given intervals in Table 3 can serve for an initial and rough estimation of the redox kinetic parameter.

The most useful analysis of the split SW peaks is obtained by varying the amplitude of the potential modulation. As shown in Figure 6 the potential separation between the split SW peaks is a linear function of the amplitude with a slope and intercept being dependent on the redox kinetics and thickness of the film. Therefore, comparing the theoretical and experimental data for the peak separation measured by altering the SW amplitude one can estimate the standard redox rate constant if the thickness of the film is known. Interestingly, SWV is able to access the kinetics of the electrode reaction in thin-film voltammetry without varying the time window of the voltammetric experiment, i.e., the SW frequency. The SW amplitude is an additional useful tool in the hands of the experimentalist, which makes this technique in many cases superior to the standard cyclic voltammetric method. In the splitting phenomenon, another important fact has to be pointed out, i.e., the splitting is stronger as the redox kinetic parameter is larger. Recalling the definition of redox kinetic parameter $K = (k_s/\sqrt{(Df)})$ it follows that large values of k_s and low values of f are favorable for the splitting. Accordingly, the kinetics of fast and reversible

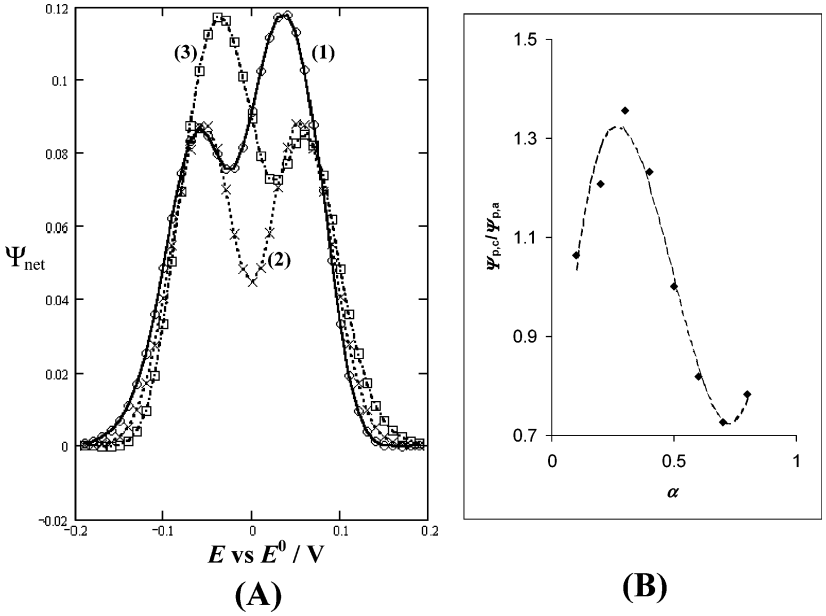

Figure 7. The effect of the electron transfer coefficient on the split SW peaks (A) and ratio of the split peak current heights (B). For A the cathodic electron transfer coefficient was $\alpha = 0.3$ (1), 0.5 (2), and 0.7 (3). The other conditions of the simulations for both A and B were redox kinetic parameter $\log(K) = -0.2$, thickness parameter $\log(\Lambda) = -0.5$, amplitude $nE_{sw} = 80$ mV, and scan increment $dE = 10$ mV.

electrode reactions can be easily measured at low frequency, i.e., at low scan rate, which is a unique ability of SWV.

Finally, Figure 7 depicts the influence of the electron transfer coefficient on the split SW peaks. Although the potential separation between split peaks is virtually unaffected by the electron transfer coefficient, the relative height of the split peaks is appreciably sensitive to α. Only for $\alpha = 0.5$ is the height of both peaks equal (see curve 2 in Figure 7A). For $\alpha < 0.5$ the ratio $\Psi_{p,c}/\Psi_{p,a} > 1$ (see curve 1 in Figure 7A), where $\Psi_{p,c}$ and $\Psi_{p,a}$ are the peak currents of the peaks appearing at more positive and more negative potentials, respectively. For $\alpha > 0.5$ the situation is the opposite (see curve 3 in Figure 7A). Figure 7B represents the complete dependence of the peak current ratio versus the electron transfer coefficient. Over the interval $0.3 \leq \alpha \leq 0.7$ the dependence of $\Psi_{p,c}/\Psi_{p,a}$ versus α is linear associated with the following equation: $\Psi_{p,c}/\Psi_{p,a} = -1.672\alpha + 1.8628$ ($R = 0.99$) which can be used for an accurate estimation of the electron transfer coefficient.

In conclusion, the splitting of the net SW response in thin-film voltammetry enables complete characterization of the kinetics of the electrode reaction as well as an accurate determination of the formal potential of the electrode reaction that is an important thermodynamic parameter, by a simple and fast procedure. For a given thickness of the film, the potential separation between the split peaks is sensitive to the kinetics of the electrode reaction being independent of the electron transfer coefficient. On the other hand, the ratio of the peak heights depends only on the electron transfer coefficient.

Acknowledgment. The financial support of A. v. Humboldt-Stiftung, Ministry of Education of Macedonia, and Universit de Bretagne Occidentale is gratefully acknowledged.

Note Added after ASAP Posting. This article was posted ASAP on 6/11/2004. A change has been made in the denominator of eq 9. The correct version was posted on 8/16/2004.

References and Notes

(1) Armstrong, A. F.; Heering, A. H.; Hirst, J. *Chem. Soc. Rev.* **1997**, *26*, 169.
(2) Hirst, J.; Armstrong, A. F. *Anal. Chem.* **1998**, *70*, 5062.
(3) Hirst, J.; Jameson, N. L. G.; Allen, W. A. J.; Armstrong, A. F. *J. Am. Chem. Soc.* **1998**, *120*, 11994.
(4) Rusling, F. J.; Forster, R. J. *J. Colloid Interface Sci.* **2003**, *262*, 1.
(5) Munge, B.; Pendon, Z; Frank, A. H.; Rusling, F. J. *Bioelectrochem.* **2001**, *54*, 145.
(6) Naumann, R.; Schmidt, E. K.; Jonczyk, A.; Fendler, K.; Kadenbach, B.; Liebermann, T.; Offenhausser, A.; Knoll, W. *Biosens. Bioelectronics* **1999**, *14*, 651.
(7) Shen, L.; Hu, N. *Biochim. Biophys. Acta* **2004**, *1608*, 23.
(8) Lu, H.; Li, Z.; Hu, N. *Biophys. Chem.* **2003**, *104*, 623.
(9) Lu, Z.; Huang, Q.; Rusling, F. J. *J. Electroanal. Chem.* **1997**, *423*, 59.
(10) Yang, J.; Hu, N.; Rusling, F. J. *J. Electroanal. Chem.* **1999**, *463*, 53.
(11) Lvov, M. Y.; Lu, Z.; Schenkman, B. J.; Zu, X.; Rusling, F. J. *J. Am. Chem. Soc.* **1998**, *120*, 4073.
(12) Zhang, Y.; Zhang, C.; Shen, H. *Electroanalysis* **2001**, *13*, 1431.
(13) Wang, Q.; Li, N.; Wu, Y. *Electroanalysis* **2001**, *13*, 149.
(14) Ciureanu, M.; Goldstein, S.; Mateescu, A. M. *J. Electrochem. Soc.* **1998**, *145*, 533.
(15) Andrieux, P. C.; Dumas-Bouchait, M. J.; Saveant, M. J. *J. Electroanal. Chem.* **1982**, *131*, 1.
(16) Albery, W. J.; Hillman, R. A. *J. Electroanal. Chem.* **1984**, *170*, 27.
(17) Chen, T.; Barton, C. S.; Binyamin, G.; Gao, Q. Z.; Zhang, Z. Y.; Kim, H. H.; Heller, A. *J. Am. Chem. Soc.* **2001**, *123*, 8630.
(18) Lyons, G. E. M.; Lyons, H. C.; Fitzgerald, C.; Bannon, T. M. *Analyst* **1993**, *118*, 361.
(19) Buttry, A. D.; Anson, C. F. *J. Am. Chem. Soc.* **1986**, *106*, 59.
(20) Karolyn, M. M.; Terrill, H. R.; Meyer, J. T.; Murray, W. R.; Wightman, M. R. *J. Am. Chem. Soc.* **1996**, *118*, *10*, 609.
(21) Shi, C.; Anson, C. F. *Anal. Chem.* **1998**, *70*, 3114.
(22) Shi, C.; Anson, C. F. *J. Phys. Chem. B* **1998**, *102*, 9850.
(23) Shi, C.; Anson, C. F. *J. Phys. Chem. B* **1999**, *103*, 6283.
(24) Chung, T. D.; Anson, C. F. *Anal. Chem.* **2001**, *73*, 337.
(25) Shi, C.; Anson, C. F. *J. Phys. Chem. B* **2001**, *105*, 1047.
(26) Shi, C.; Anson, C. *J. Phys. Chem. B* **2001**, *105*, 8963.
(27) Scholz, F.; Komorsky-Lovrić, Š.; Lovrić, M. *Electrochem. Commun.* **2000**, *2*, 112.
(28) Komorsky-Lovrić, Š.; Lovrić, M.; Scholz, F. *J. Electroanal. Chem.* **2001**, *508*, 129.
(29) Komorsky-Lovrić, Š.; Riedl, K.; Gulaboski, R.; Mirčeski, V.; Scholz, F.; *Langmuir* **2002**, *18*, 8000; **2003**, *19*, 3090.
(30) Gulaboski, R.; Mirčeski, V.; Scholz, F. *Electrochem. Commun.* **2002**, *4*, 277.
(31) Gulaboski, R.; Riedl, K.; Scholz, F. *Phys. Chem. Chem. Phys.* **2003**, *5*, 1284.
(32) Gulaboski, R.; Scholz, F. *J. Phys. Chem.* **2003**, *107*, 5650.
(33) Bouchard, G.; Galland, A.; Carrupt, P.-A.; Gulaboski, R.; Mirčeski, V.; Scholz, F.; Girault, H. *Phys. Chem. Chem. Phys.* **2003**, *5*, 3748.
(34) Mirčeski, V.; Gulaboski, R.; Scholz, F. *J. Electroanal. Chem.* **2004**, *566*, 351.
(35) Aoki, K.; Tokuda, K.; Matsuda, H. *J. Electroanal. Chem.* **1983**, *146*, 417.
(36) Lovrić, M.; Komorsky-Lovric, Š.; Scholz, F. *Electroanalysis* **1997**, *9*, 575.
(37) Aoki, K.; Tokuda, K.; Matsuda, H *J. Electroanal. Chem.* **1984**, *160*, 33.
(38) Aoki, K.; Osteryoung, J. *J. Electroanal. Chem.* **1988**, *240*, 45.
(39) Lovrić, M. In *Electroanalytical Methods, Guide to Experiments and Applications*; Scholz, F., Ed.; Springer-Verlag: Berlin; Heidelberg, 2002; pp 111−133.
(40) Mirčeski, V. *J. Electroanal. Chem.* **2003**, *545*, 29.
(41) Mirčeski, V.; Lovrić, M. *Electroanalysis* **1997**, *9*, 1283.
(42) Komorsky-Lovrić, Š.; Lovrić, M. *Anal. Chim. Acta* **1995**, *305*, 248.
(43) Mirčeski, V.; Lovrić, M.; Jordanoski, B. *Electroanalysis* **1999**, *11*, 660.
(44) Mirčeski, V.; Lovrić, M. *Anal. Chim. Acta* **1999**, *386*, 47.
(45) Mirčeski, V.; Lovrić, M. *Electroanalysis* **1999**, *11*, 984.
(46) Komorsky-Lovrić, Š.; Lovrić, M. *J. Electroanal. Chem.* **1995**, *384*, 115.
(47) Lovrić, M.; Komorsky-Lovrić, Š. *J. Electroanal. Chem.* **1988**, *248*, 239.
(48) Lovrić, M.; Mlakar, M. *Electroanalysis* **1995**, *7*, 1121.
(49) Mirčeski, V.; Gulaboski, R.; Jordanoski, B.; Komorsky-Lovrić, Š. *J. Electroanal. Chem.* **2000**, *490*, 37.